TECHNICAL NOTE

Radiation Medicine: Vol. 22 No. 4, 275–282 p.p., 2004

Diffusion Weighted Whole Body Imaging with Background Body Signal Suppression (DWIBS): Technical Improvement Using Free Breathing, STIR and High Resolution 3D Display

Taro Takahara,* Yutaka Imai,* Tomohiro Yamashita,* Seiei Yasuda, Seiji Nasu,* and Marc Van Cauteren*****

Purpose: To examine a new way of body diffusion weighted imaging (DWI) using the short TI inversion recovery-echo planar imaging (STIR-EPI) sequence and free breathing scanning (diffusion weighted whole body imaging with background body signal suppression; DWIBS) to obtain three-dimensional displays.

Materials and Methods: 1) Apparent contrast-to-noise ratios (AppCNR) between lymph nodes and surrounding fat tissue were compared in three types of DWI with and without breath-holding, with variable lengths of scan time and slice thickness. 2) The STIR-EPI sequence and spin echo-echo planar imaging (SE-EPI) sequence with chemical shift selective (CHESS) pulse were compared in terms of their degree of fat suppression. 3) Eleven patients with neck, chest, and abdominal malignancy were scanned with DWIBS for evaluation of feasibility. Whole body imaging was done in a later stage of the study using the peripheral vascular coil.

Results: The AppCNR of 8 mm slice thickness images reconstructed from 4 mm slice thickness source images obtained in a free breathing scan of 430 sec were much better than 9 mm slice thickness breath-hold scans obtained in 25 sec. High resolution multi-planar reformat (MPR) and maximum intensity projection (MIP) images could be made from the data set of 4 mm slice thickness images. Fat suppression was much better in the STIR-EPI sequence than SE-EPI with CHESS pulse. The feasibility of DWIBS was showed in clinical scans of 11 patients. Whole body images were successfully obtained with adequate fat suppression.

Conclusion: Three-dimensional DWIBS can be obtained with this technique, which may allow us to screen for malignancies in the whole body.

Key words: DWIBS, diffusion weighted images, whole body imaging, STIR, cancer screening

INTRODUCTION

RECENT ADVANCES IN MR GRADIENT TECHNOLOGY ALLOW acquisition of diffusion-weighted images with high b-factor even in the body, thanks to the advent of fast imaging sequences like echo planar imaging (EPI) and parallel imaging techniques like sensitivity encoding (SENSE).[1,2] Previously reported results show great potential for the detection of pathological lesions.[3-5] This strategy is similar to positron emission tomography (PET) imaging. However, it is difficult to obtain PET-like three-dimensional images with a large field of view because of two major limitations.

One of the limitations is the brief scan time, which leads to poor image quality. As diffusion weighted imaging (DWI) theoretically aims to detect motion over very small distances, such as Brownian motion, breath-hold scan has been considered the only way to avoid the artifacts from the bulk motion of subjects. The limitation of scan time by breath hold does not permit thin slice DWI with adequate signal-to-noise ratio (SNR) and multiple excitations that can be used as source images of three-dimensional display.

The other limitation is insufficient fat suppression

Received April 9, 2004; revision accepted July 29, 2004.

Departments of *Radiology and **Gastroenterological Surgery, Tokai University School of Medicine

***Philips Medical Systems

Reprint requests to Taro Takahara, Department of Radiology, Tokai University School of Medicine, Bouseidai, Isehara-shi, Kanagawa 259-1193, JAPAN.

Table 1. Imaging parameters of four types of DWI

Type of scan	Breath-hold 9 mm	Non-breath-hold 9 mm	Non-breath-hold 4 mm	Non-breath-hold whole body
Sequence	SE-EPI	STIR-EPI	STIR-EPI	STIR-EPI
Mode	Single shot	Single shot	Single shot	Single shot
Coil	SENSE body	SENSE body	SENSE body	Peripheral vascular
Slice orientation	Axial	Axial	Axial	Axial
TR (ms)	1612	2969	5122	6660
TE (ms)	60	70	70	70
TI (ms)	180	180	180	180
SPIR	Yes	No	No	No
FOV (mm)	400	400	400	400
RFOV% (%)	70	70	70	70
Matrix	160	160	160	160
Scan percentage (%)	80	80	80	80
Half scan factor	0.6	0.6	0.6	0.6
EPI factor	47	47	47	47
SENSE factor	2	2	2	2
MPG	3 axis	3 axis	3 axis	Phase only
b-facor	500	1000	1000	1000
NEX	2	10	10	12
Number of slices	15	15	60	80
Slice thickness (mm)	9	9	4	6
Slice gap (mm)	1	1	−1(overlap)	−1(overlap)
Acquisition time (sec)	25	124	430	346

Abbreviations: STIR; Short TI inversion recovery, TR; Repetition time, TE; Echo time, TI; Inversion time, SPIR; Spectral presaturation with inversion recovery, FOV; Field of view, RFOV; Rectangular FOV percentage, SENSE; Sensitivity encoding, MPG; Motion probing gradient, NEX; Number of excitations.

when using the usual combination of the spin echo-echo planar imaging (SE-EPI) sequence and chemical shift selective (CHESS) technique. When displayed in 2D, insufficient fat suppression that appears in the peripheral portions of the image does not have a severe effect on image interpretation and does not hamper the diagnosis. However, in 3D display, residual fat signal in the periphery of the subject will be superimposed on the central portions of the body, possibly obscuring important lesions inside the body.

We have developed a new way to obtain multiple thin slice DWI using 1) a free breathing approach that affords multiple slice excitations and signal averaging over an extended period of time, and 2) a short TI inversion recovery (STIR)-EPI sequence that allows potent fat suppression, which may improve the quality of the 3D reconstructed images in whole body imaging. The purpose of this article is to describe this method and to assess the potential of lesion detection in three-dimensional displays of DWI data.

MATERIALS AND METHODS

We evaluated the following three items: 1) Comparison of breath-hold vs. free breathing methods using the apparent contrast-to-noise ratio (AppCNR) between lymph nodes and surrounding fat tissue in five patients who had an upper abdominal scan; 2) comparison of SE-EPI with chemical shift selective fat suppression (SPIR) pre-pulses vs. STIR-EPI using the degree of fat suppression in five patients who had a scan of the upper chest to neck region; 3) feasibility of STIR-EPI diffusion weighted imaging in 11 patients with neck, chest, and abdominal malignancy. Later in the study, we attempted whole body diffusion weighted scanning using the peripheral vascular coil.

All images were obtained on a 1.5 Tesla Gyroscan Intera MR scanner (gradient strength=33 mT/m, slew rate=160 T/m/s, Philips Medical Systems, Best, The Netherlands). The imaging parameters used for each of the sub-studies are listed in Table 1. Details of the three studied items are as follows.

Comparison of breath-holding and free breathing scan

As described in the introduction, thin-slice DWI had to be obtained with comparable signal and contrast to thick-slice 2D DWI during breath-hold. Therefore, we compared the CNR of lymph nodes and surrounding fat tissue measured with the following three different types

of DWI: i) 9 mm slice thickness DWI using a b-value of 500 sec/mm^2 obtained during a breath-hold (25 sec); ii) 9 mm slice thickness DWI using a b-value of 1,000 sec/mm^2 during free breathing (124 sec) and iii) 8 mm slice thickness reconstructed DWI using a b-value of 1,000 sec/mm^2 obtained from 4 mm slice thickness during free breathing (430 sec). With a breath-hold scan, selection of a b-value over 500 sec/mm^2 was not practical because acceptable image quality could not be obtained due to the limited number of signal averagings during the breath-holding period. Multi-planar reconstruction was done with the standard multi-planar reformat (MPR) function of the Gyroscan Intera system.

AppCNR was defined and calculated using the following equation:

AppCNR=([SI $_{lym}$]−[SI $_{fat}$]) / [SD $_{fat}$], where [SI $_{lym}$] is the signal intensity of the lymph nodes and [SI $_{fat}$] is the signal intensity of fat. [SD $_{fat}$] is the standard deviation of the signal intensity within the regions of interest (ROI).

AppCNR will be high when ([SI $_{lym}$]−[SI $_{fat}$]) is high or [SD $_{fat}$] is low. A high value of ([SI $_{lym}$]−[SI $_{fat}$]) corresponds to a large difference of signal intensity in the two adjacent ROIs, one covering the lymph node and the other covering the adjacent fat. Also, a low value of [SD $_{fat}$] reflects a small fluctuation of signal intensity in the surrounding fat tissue. Therefore, a high value of AppCNR, that is ([SI $_{lym}$]−[SI $_{fat}$]) / [SD $_{fat}$] , indicates good image quality.

ROI for the lymph nodes were placed on the three largest lymph nodes in each volunteer. It was unknown whether these selected lymph nodes had metastasis or inflammation, or neither. However, the same lymph nodes were evaluated in each scan. The shape of the ROI was elliptical and was fitted to the shape of the lymph nodes. The ROI of fat was placed adjacent to the selected lymph nodes and had a circular shape with the same diameter. The average values and standard deviations of the AppCNR were calculated for each type of scan.

Comparison of SE-EPI with chemical shift selective fat suppression (SPIR) pre-pulses vs. STIR-EPI

In general, a SPIR pulse is employed in DWI in combination with an SE-EPI sequence. This technique works well for the central nervous system (CNS) and even in the body, as long as 2D acquisition is used. However, more accurate fat suppression is required in 3D display especially in the peripheral area of the field of volume (FOV) because the remaining fat signal in the peripheral area of the FOV could obscure signal in the central part of the body when using a 3D approach. As is well known, the STIR pre-pulse (a hyperbolic secant adiabatic inversion pulse) gives superior results compared to sequences with the CHESS pre-pulse for fat suppression over an extended FOV. Therefore, we think STIR could be necessary when acquiring data suitable for 3D display covering a very large FOV.

This led us to compare SE-EPI using the SPIR pre-pulse with STIR-EPI, in five patients that underwent a scan of the upper chest to neck region. The evaluation was done using a three-point scale (i.e., good, fair, and poor) of fat suppression efficiency evaluated on maximum intensity projection (MIP) imaging by the consensus of two board-certified radiologists. “Good” means that fat suppression is perfect. “Fair” means that fat suppression is slightly poor, but central organs and tissues can be evaluated. “Poor” means that fat suppression is poor and central objects were obscured.

Feasibility of STIR-EPI diffusion weighted imaging as a tool to visualize malignancy in 3D

We evaluated the feasibility of thin slice STIR-EPI diffusion weighted imaging and its 3D display in a total of 11 patients. The subjects included patients with malignant lymphoma (n=5), recurrent rectal cancer (n=2), breast cancer (n=2), esophageal cancer (n=1), and ovarian cancer (n=1). In two patients with recurrent rectal cancer and one with ovarian cancer, DWI was compared with a PET scan. In one patient with malignant lymphoma, two examinations were performed with an interval of three months. In a later stage of the study, we attempted whole body scanning in three patients with malignant lymphoma. For three-dimensional display, MIP was employed using a black and white inverse gray scale.

RESULTS

1) AppCNR of lymph nodes in 9 mm slice thickness free breathing scans was higher than that of 9 mm slice thickness breath-hold scans (Table 2), and 8 mm slice thickness reconstructed images calculated from 4 mm slice thickness scans obtained in 430 sec had comparable AppCNR with 9 mm slice thickness scans obtained in 124 sec. Therefore, high resolution MPR images and 3D displays using the MIP algorithm could be obtained using the 4 mm slice thickness source images (Fig. 1).

2) All subjects showed “good” fat suppression on DWI obtained by STIR-EPI. On the other hand, DWI obtained by SE-EPI with SPIR was “fair” in only one patient and “poor” in four patients (Fig. 2).

3) In the feasibility study on patients with malignancy, excellent results were obtained. In the case of breast cancer and esophageal cancer, three-dimensional distributions of the advanced primary lesion and

Table 2. Apparent contrast-to-noise ratio measured in three types of DWI

Type of scan	Breath-hold 9 mm th.	Free breathing 9 mm th.	Free breathing 4 mm th. Reconstructed to 8 mm th.
AppCNR (±SD)	18.1±9.6	41.5±19.8	44.8±20.8

Abbreviations: AppCNR; Apparent contrast-to-noise ratio, SD; Standard deviation, th; thickness

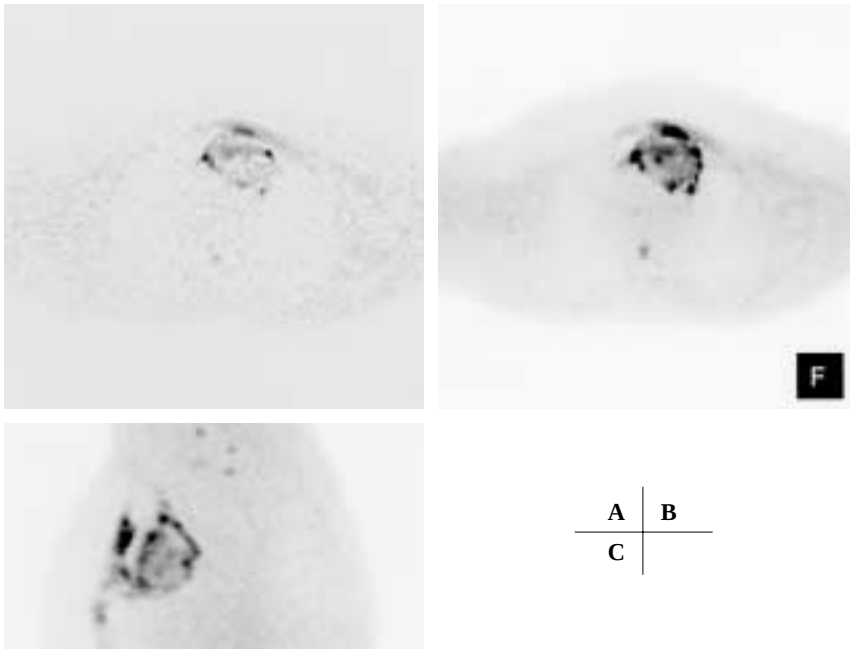

Fig. 1. Comparison between breath-hold scan and non-breath-hold scan in a 23-year-old man with thymoma.
A: A 9 mm-thick axial image obtained with 25 sec breath-hold scan.
B: An 8 mm-thick reconstructed axial image calculated from 4 mm-thick axial image obtained with 430 sec non-breath-hold scan.
C: A 5 mm-thick sagittal reconstructed image calculated from 4 mm-thick axial image.
SNR of non-breath-hold scan (B) is much better than that of breath-hold scan (A). High resolution MPR image can be obtained using B (C).

Fig. 2. Comparison of STIR-EPI and SE-EPI with CHESS pulse in degree of fat suppression in a 28-year-old man with swollen lymph nodes (pathology unknown).
A: MIP image obtained by SE-EPI sequence with CHESS pulse.
B: MIP image obtained by STIR-EPI sequence.
SE-EPI DWI with CHESS pulse (A) shows insufficient fat suppression around the jaw and clavicle. On the other hand, STIR-EPI DWI shows evidence of adequate fat suppression. Swollen lymph nodes around the left submandibular gland (*arrow*) are well visualized without interfering artifact.

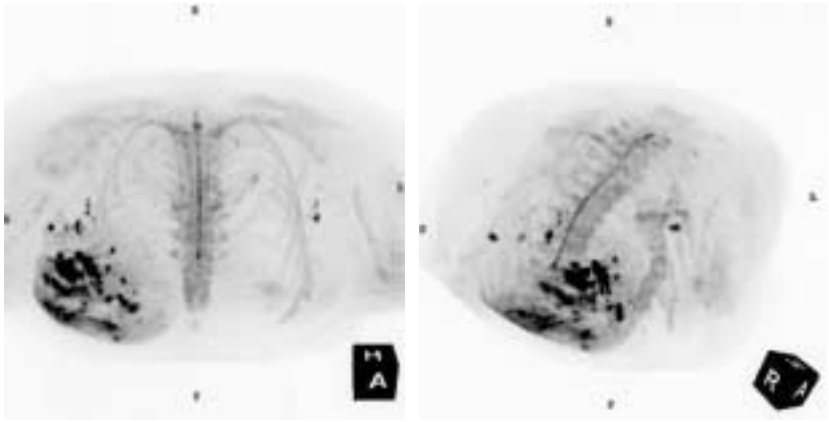

Fig. 3. A 76-year-old woman with advanced breast cancer.
A: MIP image from antero-superior viewpoint.
B: MIP image from right antero-superior viewpoint.
A large breast cancer located in right breast is demonstrated as a low intensity area. Associated inflammatory process is seen around the tumor. Axillar lymph node metastasis is well visualized. Although the shoulder is one of the frequent sites where fat suppression tends to be insufficient, the effect of fat suppression is excellent.

A | B

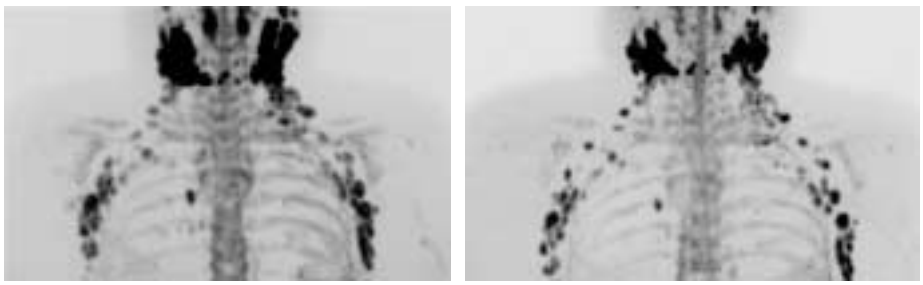

Fig. 4. A 69-year-old woman with malignant lymphoma.
A: Before chemotherapy.
B: After chemotherapy. Three months after A.
Severe swelling and fusion of lymph nodes are demonstrated before chemotherapy. After chemotherapy, these lymph nodes are separated. The slight improvement is well recognized in comparison with only single MIP images in each study.

A | B

metastatic lymph nodes were clearly demonstrated with excellent fat suppression (Fig. 3). In cases of malignant lymphoma, swollen lymph nodes were well visualized. In one case that underwent two examinations of DWI before and after chemotherapy, the change was well understood on MIP images (Fig. 4). In one case of a 4-year-old child, the image quality was adequate for diagnosis even though the scan was done without breath-hold (Fig. 5). In one case of peritoneal dissemination from ovarian cancer, the peritoneal nodules were well visualized, and were clearer than on contrast enhanced CT (Fig. 6). In three cases of malignancy that also underwent PET scan, DWI precisely indicated the site of malignant tumor, and it was more sharply demonstrated than with PET (Fig. 7). Whole body scanning using the peripheral vascular coil was performed successfully, and the acquired images

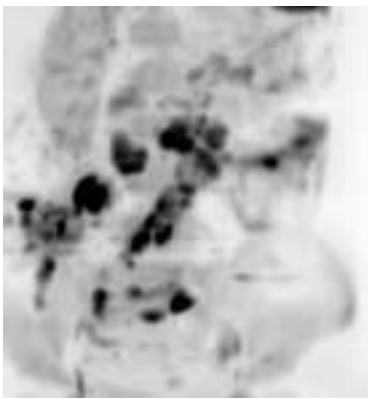

Fig. 5. A 4-year-old boy with malignant lymphoma.
Coronal MIP image of DWI. Distribution of swollen mesenteric lymph node is well evaluated even in a child who cannot cooperate well during the breath-holding examination.

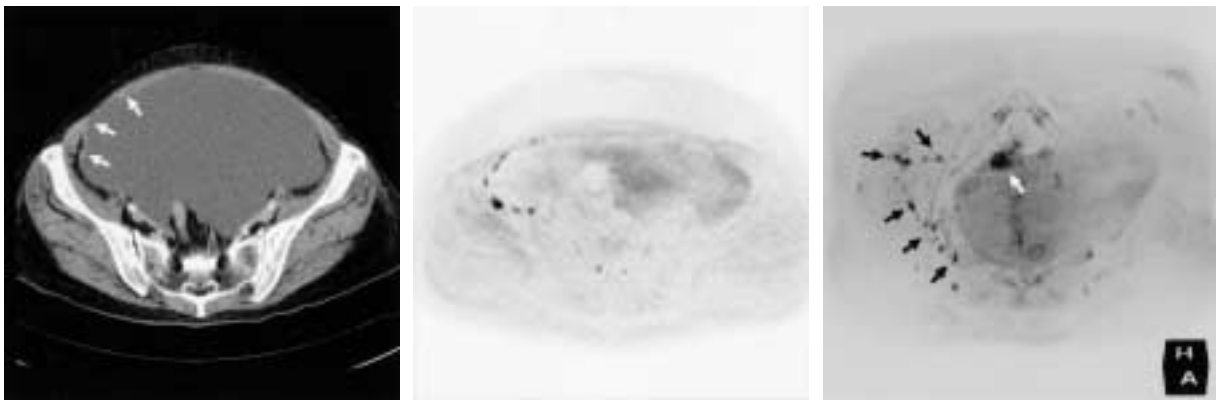

Fig. 6. A 64-year-old woman with ovarian cancer and peritoneal dissemination.
A: Contrast enhanced CT.
B: DWI.
C: MIP image of DWI from antero-superior viewpoint.
Multiple small nodules along the peritoneum are demonstrated, suggesting peritoneal dissemination (*arrows,* A). DWI shows these nodules more clearly. Three-dimensional distributions of lymph nodes along right abdominal wall can be evaluated in MIP image (*arrows,* C) with visualization of primary lesion (*white arrow*).

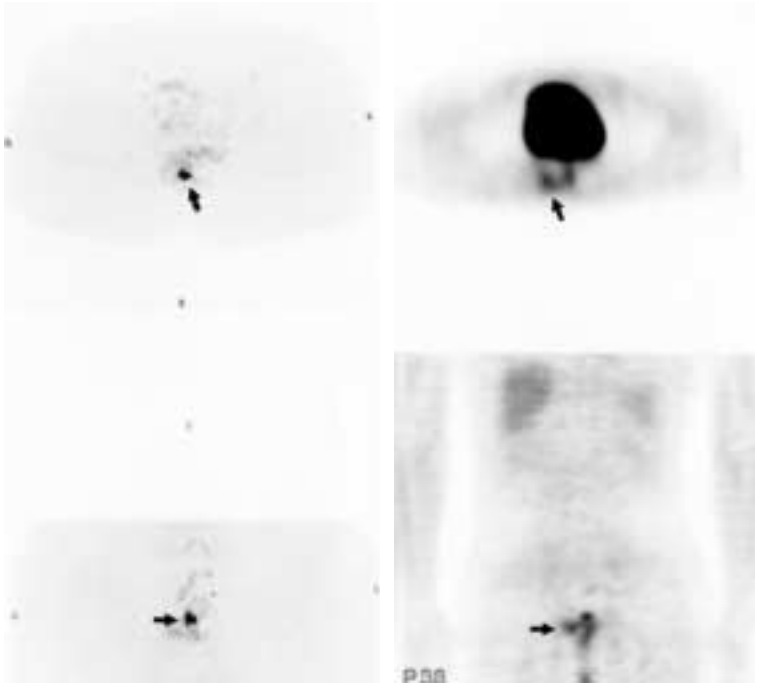

Fig. 7. A 60-year-old man with recurrent rectal cancer.
A: DWI, axial image.
B: DWI, coronal MIP image.
C: PET scan, axial image.
D: PET scan, coronal image.
DWI (inverted gray/white scale) shows abnormal low intensity area just lateral to the anastomosis (*arrows,* A and B). PET confirmed recurrent tumor in the same portion (*arrows,* C and D), but spatial resolution is inferior to DWI.

depicted extensive spreading of swollen lymph nodes (Fig. 8).

DISCUSSION

Diffusion weighted imaging is now widely used in imaging the central nervous system, especially in cases of acute stroke.[6] Lesions imaged shortly after an infarction showed a decreased degree of diffusion, as indicated by the apparent diffusion coefficient (ADC), compared with that of normal tissue. Therefore, DWI depicts acute infarction as a high signal intensity area. Several researchers have already reported that various malignancies in the body show similar high signal intensity,[3-5] but the reason for this is unknown. Nomura *et al.* noted that the cellularity of a lesion was related to its ADC value in their study of bone marrow in a limited number of cases.[7] Since a malignant tumor often has a larger cell diameter and denser cellularity than normal tissue, the ADC of tumors may be decreased. Further

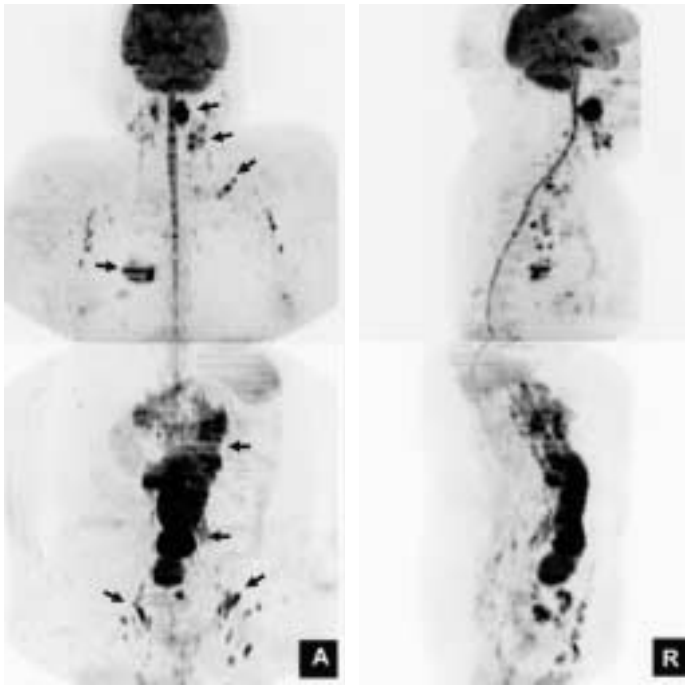

A | B

Fig. 8. A 55-year-old woman with malignant lymphoma under whole body scan with peripheral vascular coil.
A: Coronal MIP image.
B: Sagittal MIP image.
Eighty cm coverage of DWI enables visualization of whole body distribution of swollen lymph nodes in Wardyer's ring, left sided neck, supraclavicular, chest, mesenteric, and inguinal portions (*arrows*).

evaluation of this conjecture remains to be done. However, our study suggests the potential capability of DWI as a screening tool for malignancy. This is due to good background body signal suppression including vessel, muscle, and fat signal by the heavy diffusion weighting and/or the STIR pulse.

2-[Fluorine-18]-fluoro-2-deoxy-D-glucose (^{18}FDG)-PET has been developed recently, and it is now used as a powerful screening tool for malignancy.[8] As PET images are obtained as axial slices like CT, three-dimensional display or MPR can be done easily. This is convenient for analyzing the distribution of primary lesions and their metastases.

From the standpoint of whole body malignancy screening, until now, a significant limitation of diffusion weighted imaging has been that it used thick slices and the fat suppression was not reliable. Thin slices are necessary for 3D display, but slice thickness was limited because a breath-hold scan to avoid physiological motion was used.

However, we have shown that free breathing scanning works very well. Longer scan time affords more slices with multiple signal averaging, higher SNR, and potent fat suppression, enabling quality MIP reconstruction.

The reason why the non-breath-hold method works is not yet fully understood. We hypothesize that, when a pair of motion probing gradients (MPGs) are applied to moving objects, they will not yield any significant signal. Therefore, it seems controversial to use MPG for body imaging during free breathing. However, considering normal breathing motion, the subject is not always moving and there are significantly long stable periods. The MPGs are applied within a very small time interval of about 50 ms (i.e., less than the echo time). Therefore, a pair of MPGs applied in the stable period will yield signal. As we use multi-excitation for data acquisition, some signal will be acquired during this "stable" period during the breathing cycle. Furthermore, signal averaging is performed on the reconstructed images, and not in k-space. Therefore we do not have destructive phase effects that would ruin the eventual image. This hypothesis was not verified in this study, and further evaluation is required.

We have shown that STIR produces excellent fat suppression even when using EPI-DWI in the body. Therefore, two significant limitations as described above have been overcome. A preliminary result of our feasibility study suggests that 3D body DWI has great potential as a novel tool for evaluating pathological lesions including malignancy. Its images–displayed with an inverted gray-white scale–also seem familiar to clinicians, as they have some resemblance to the usual displays seen in scintigraphy or in PET.

The reason we used STIR was to obtain complete fat suppression, as mentioned previously. However, STIR may affect image contrast. Mazumdar *et al.*[9] have described the efficacy of the STIR pre-pulse in their series of pediatric malignancy diagnosed by means of whole body MR imaging. They found that STIR was less specific than T1-weighted or T2-weighted imaging,

because the T1 and T2 components were additive in STIR. Nonetheless, it was useful for the detection of lesions because most of the pathologic lesions had increased free water, and thus prolonged T1 and T2 values, resulting in a bright signal on STIR.

STIR may be useful in suppressing the intestinal signal that has a short T1 value. However, SNR is lower in STIR than in SE. This means that STIR tends to be a time-consuming process. Therefore, when scan time is limited, SE can be selected although fat suppression may be incomplete.

There are two limitations to our study. First, the AppCNR we used in this study is not a standard index to reflect CNR. On a SENSE image, the real SNR cannot be measured in a simple straightforward way for two reasons. First, the SNR varies from pixel to pixel as determined by the geometry factor. Second, the regularization algorithm will force the signal intensity and standard deviation of pixels outside the body to be zero. Therefore, we used an "apparent contrast to noise ratio (AppCNR)" in this evaluation. Another limitation is that we have not determined the specificity of DWI. In our experience, DWI tends to have poor specificity in detecting lesions. Further evaluation is necessary on this point. Additionally, image acquisition under free breathing may affect spatial resolution.

In spite of the drawbacks addressed above, DWI seems to have several advantages over PET scanning. First of all, it involves no ionizing radiation; furthermore, it does not require large facilities such as a cyclotron, and therefore costs much less (approximately one-sixth on a reimbursement basis in Japan) than PET scanning. Therefore, DWI may be used as a screening tool.

CONCLUSION

High resolution diffusion-weighted MR imaging with the STIR-EPI sequence and free breathing scanning provides multiple signal averages as well as adequate fat suppression, and can be used to create optimum 3D display. We believe that this technique offers significant improvement for whole body screening strategies with diffusion weighted imaging.

ACKNOWLEDGEMENTS

We thank Isao Muro, R.T., Akira Hanaki, R.T., Tomohiko Horie, R.T., and Kyoko Tomiyasu, R.T. for clinical operation of MR imaging and technical advice. We also thank Rica Tanaka, M.D. for preparing the English manuscript.

REFERENCES

1) Willinek WA, Gieseke J, von Falkenhausen M, Neuen B, Schild HH, Kuhl CK. Sensitivity encoding for fast MR imaging of the brain in patients with stroke. *Radiology*, 228: 669–675, 2003.
2) Cercignani M, Horsfield MA, Agosta F, Filippi M. Sensitivity-encoded diffusion tensor MR imaging of the cervical cord. *AJNR Am J Neuroradiol*, 24: 1254–1256, 2003.
3) Ichikawa T, Araki T. Fast magnetic resonance imaging of liver. *Eur J Radiol*, 29: 186–210, 1999.
4) Guo Y, Cai YQ, Cai ZL, Gao YG, An NY, Ma L, Mahankali S, Gao JH. Differentiation of clinically benign and malignant breast lesions using diffusion-weighted imaging. *JMRI*, 16: 172–178, 2002.
5) Kinoshita T, Yashiro N, Ihara N, Funatu H, Fukuma E, Narita M. Diffusion-weighted half-Fourier single-shot turbo spin echo imaging in breast tumors: differentiation of invasive ductal carcinoma from fibroadenoma. *J Comput Assist Tomogr*, 26: 1042–1046, 2002.
6) Huisman TA. Diffusion-weighted imaging: basic concepts and application in cerebral stroke and head trauma. *Eur Radiol*, 13: 2283–2297, 2003.
7) Nonomura Y, Yasumoto M, Yoshimura R, Haraguchi K, Ito S, Akashi T, Ohashi I. Relationship between bone marrow cellularity and apparent diffusion coefficient. *J Magn Reson Imaging*, 13: 757–760, 2001.
8) Rohren EM, Turkington TG, Coleman RE. Clinical applications of PET in oncology. *Radiology*, 231: 305–332, 2004.
9) Mazumdar A, Siegel MJ, Narra V, Luchtman-Jones L. Whole-body fast inversion recovery MR imaging of small cell neoplasms in pediatric patients: a pilot study. *AJR Am J Roentgenol*, 179: 1261–1266, 2002.